Chemical Engineering Journal 101 (2004) 143–149

Chemical Engineering Journal

www.elsevier.com/locate/cej

MEMS-based components of a miniature fuel cell/fuel reformer system

Shuji Tanaka [a,*], Kuei-Sung Chang [a], Kyong-Bok Min [a], Daisuke Satoh [a], Kazushi Yoshida [b], Masayoshi Esashi [c]

[a] *Department of Mechatronics and Precision Engineering, Tohoku University, 01 Aza Aoba, Aramaki, Aoba-ku, Sendai 980-8579, Japan*
[b] *Matsushita Electric Works Ltd., Japan*
[c] *New Industry Creation Hatchery Center, Tohoku University, Japan*

Abstract

The components of a novel miniature fuel cell/fuel reformer system fueled by liquid gases such as butane and propane were prototyped by MEMS technology and tested. In this system, fuel, air and water are supplied to the fuel reformer by utilizing the vapor pressure of the liquid gas for the reduction of power consumption by peripherals and the simplification of the system. The system is composed of a reforming reactor, a catalytic combustor, a polymer electrolyte fuel cell (PEFC), an ejector to supply air to the combustor and other peripherals. The reforming reactor demonstrated the steam reforming of methanol at an equivalent power of 200 mW and a total efficiency of 6%. The combustor had a stable combustion area above 5 W, and the complete combustion of butane was confirmed by gas chromatography. The ejector showed a potential to supply air required for the complete combustion of butane (31 times larger volume than butane). The PEFC worked, but only at low power density of about 0.1 mW/cm^2 due to poor adhesion between a polymer electrolyte membrane (PEM) and catalytic electrodes.
© 2004 Elsevier B.V. All rights reserved.

1. Introduction

Liquid hydrocarbon fuels contains enormous energy per volume and weight compared to the best existing batteries. For example, the energy density of a lithium ion battery is practically about 200 Wh/l or 100 Wh/kg, while that of gasoline reaches 13 kWh/l or 15 kWh/kg. This suggests that energy conversion efficiency of several percentage is enough for liquid hydrocarbon fuel-based power sources to overcome the energy density of existing lithium ion batteries. These power sources can be continuously used just by refueling without time-consuming recharging. Refueling is more convenient than recharging for who need portable information electronics all day and mobile robots used in disaster areas, construction sites, etc. where commercial wired electrical power is not available. Additionally, replacing batteries with recyclable fuel cartridges is environmentally friendly, because used batteries are generally difficult to be recycled, although it gives rise to environmental pollution when discarded.

From the above reasons, various challenges are recently being conducted to convert liquid hydrocarbon fuels to electrical power at micro-scale. For example, gas turbine generators [1–4], fuel cells [5–10], fuel reformers [11–13], thermoelectric generators [14,15], a thermophotovoltaic generator [16] and a thermoionic generator [17] are being miniaturized for applications such as portable electronics and mobile machines. Among them, a miniature fuel cell system combined with a micro-fuel reformer seems one of promising candidates to power laptop computers, video camcorders, etc. The miniature fuel cell/fuel reformer system is expected to become a more compact system compared to a direct methanol fuel cell (DMFC) system, because a hydrogen-fueled polymer electrolyte fuel cell (PEFC) has approximately one order of magnitude higher power density than a DMFC. Additionally, it has potential to be fueled by various hydrocarbons including methanol, ethanol, butane and dimethyl ether.

The micro-fuel reformer basically has a system configuration similar to conventional fuel reformers, consisting several key components such as a reforming reactor, a CO separator, a heat source and fluid control peripherals. In the micro-fuel reformer, these components should be as small as possible and of low power consumption. In this study, we prototyped MEMS-based components of the miniature fuel cell/fuel reformer system.

2. System concept

Fig. 1 shows the configuration of the miniature fuel cell/fuel reformer system, which produces hydrogen from

* Corresponding author. Tel.: +81-22-217-6937; fax: +81-22-217-6935.
E-mail address: shuji@cc.mech.tohoku.ac.jp (S. Tanaka).

1385-8947/$ – see front matter © 2004 Elsevier B.V. All rights reserved.
doi:10.1016/j.cej.2004.01.017

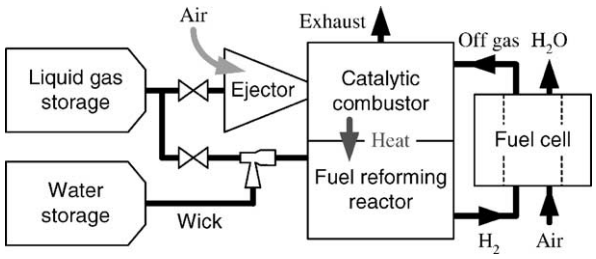

Fig. 1. Configuration of the miniature fuel cell/fuel reformer system.

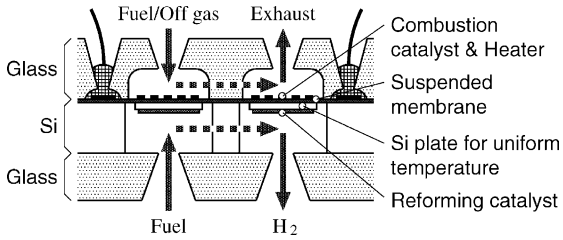

Fig. 2. Schematic structure of the micro-fuel reformer.

liquid gases such as butane and propane by steam reforming and supplies hydrogen to a PEFC. This system is composed of the PEFC, a reforming reactor, a catalytic combustor, an ejector to supply air to the combustor and peripherals. The reforming reactor is equipped with a water-shift reactor to remove CO or a palladium membrane hydrogen separator, if necessary. The advantage of using liquid gases as fuel is that the fuel, air and water can be supplied without a micro-pump by utilizing the vapor pressure of the liquid gas. Generally, micro-pumps consume, relatively, large power as well as have difficulty in ensuring reliability due to moving parts. Additionally, using micro-pumps increases the number of components, resulting in system complexity. The system which we propose is based on the novel concept that we eliminate micro-pumps to supply fuel, air and water by utilizing the vapor pressure of liquid gases.

Our system needs the development of particular components not found in a conventional micro-fuel reformer using methanol as fuel. The problems which we should first challenge are following.

(1) The reforming temperature of liquid gases is several hundreds °C, higher than that of methanol (200–300 °C), so that the excellent thermal insulation of reaction areas is essential for high total efficiency.
(2) The steam reforming of liquid gas is more difficult than that of methanol due to coking especially at low S/C (steam/carbon) ratio, so that high performance catalyst should be developed with technology for applying the catalyst to a micro-reactor.
(3) Large amount of air is necessary for the complete combustion of liquid gases. For example, butane needs air with 31 times larger volume than itself for complete combustion. The ejector should supply such a large amount of air to the combustor.
(4) The combustion of liquid gases is more challenging than that of hydrogen and methanol at micro-scale. Additionally, minimizing the pressure loss of the combustor is essential to use the ejector.

3. Combustor-integrated micro-fuel reformer

As well known, surface per volume increases with decrease in scale. This scaling effect gives rise to advantages such as rapid heating and cooling, and increase in the relative surface of catalyst. Contrarily, this scaling effect tends toward relatively large heat dissipation resulting in low thermal efficiency, if the system needs heating. In the micro-fuel reformer, to increase total efficiency is one of the most important requirements, so that thermal insulation becomes one of the most important concerns. For thermal insulation, we propose a suspended membrane structure. Fig. 2 illustrates the schematic structure of the micro-fuel reformer. The upper and lower sides of the suspended membrane are used for fuel reforming and catalytic combustion, respectively. By localizing reactions on the suspended membrane, good thermal insulation, low thermal capacity and large thermal conductance between the reforming reactor and the catalytic combustor become possible. The suspended membrane is made of a low-stressed SiO_2 membrane and a silicon center plate on it. The SiO_2 membrane with low thermal conductivity decreases heat conduction to an outer frame, and the silicon plate with high thermal conductivity prevents hot spots, which results in the break of micro-heaters.

Fig. 3 shows the prototyped micro-fuel reformer. The suspended SiO_2 membrane with a thickness of 3 μm is formed in 300 μm wide micro-channels. The membrane is fabricated by deep reactive ion etching (RIE) from the back side of the silicon substrate, following the chemical vapor depo-

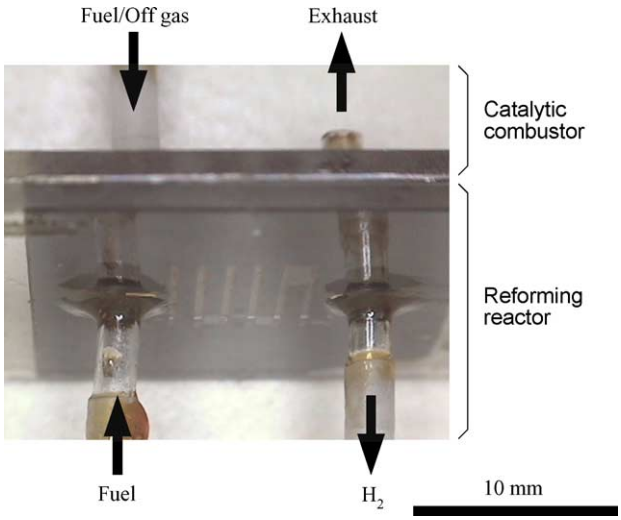

Fig. 3. Prototyped micro-fuel reformer.

sition (CVD) of SiO_2 on the front side and the patterning of Pt/Ti micro-heaters on it. Subsequently, Pyrex glass substrates with micro-channels and/or gas ports are anodically bonded to the silicon substrate.

In this study, copper, which is generally used as catalyst for methanol steam reforming, was sputter-deposited to the micro-channels as reforming catalyst. In a final goal, we will perform the steam reforming of liquid gases, but in this study, we selected the steam reforming of methanol to simply confirm the thermal insulation effectiveness of the suspended membrane. The micro-heaters were used as a heat source to replace the micro-catalytic combustor. The power required for heating the micro-channel with a width of 300 μm and a length of 7 mm to 300 °C is as low as 0.64 W. At that time, the heated area was confined just on the suspended membrane, and the outer frame surrounding the micro-channel was kept approximately at room temperature. From these results, the thermal insulation effectiveness of the suspended membrane was confirmed.

The steam reforming of the methanol was performed by the following method. First, the sputtered copper catalyst was reduced by 10 wt.% hydrogen in argon at 250 °C for 2 h. After carefully purging the micro-channel by argon, methanol mixed with water (methanol/water molar ratio 1) was supplied to the reforming reactor using a syringe pump at a feeding ratio of 5 μl/min. During reforming, the temperature of the micro-heaters was maintained at 180 °C. Reformed gas was sampled and analyzed by gas chromatography (Shimadzu, GC-14B with Shincarbon-T packed column). The measured concentration of hydrogen in the reformed gas was 24%, corresponding to a conversion ratio of 19% and an equivalent power of 200 mW. The total efficiency, η_c, which is defined by the following equation was 6%:

$$\eta_c = \frac{\text{equivalent energy of produced hydrogen}}{\text{equivalent energy of supplied methanol} + \text{energy consumed by the micro-heater}} \quad (1)$$

The low total efficiency was partly attributed to the low activity of the sputtered copper catalyst.

The integrated-catalytic combustor was also tested. Platinum-loaded TiO_2 is embedded to the combustor by the *in situ* oxidization and reduction of catalyst sol injected into the micro-channel. By this method, however, surfaces other than the suspended membrane are also coated with the catalyst, resulting in thermal loss. Thus, we are developing screen printing technology to pattern the catalyst. Combustion was first confirmed using hydrogen as fuel. By feeding 10.1 sccm hydrogen and 69.3 sccm air, combustion spontaneously started without heating using the micro-heater, and was stabled at about 100 °C. The temperature was measured using the micro-heater as a thermometer. Hydrogen flow of 10.1 sccm 1.65 W heat by complete combustion, while only 0.15 W electrical power is enough to heat the suspended membrane at 100 °C using the micro-heater. This result suggests that the combustion efficiency was still low, and that considerable heat dissipation occurred due to the above-mentioned catalyst coating method based on sol injection.

4. Micro-ejector

The micro-ejector is an essential component to exclude micro-pumps from the miniature fuel cell/fuel reformer system. The ejector sucks a secondary flow by pressure drop and dragging effect caused by the jet of a primary flow, and is used for supplying air to a burner and evacuating air from a large chamber. In our system, the primary flow is vaporized liquid gas, and the secondary flow is air. The liquid gas is ejected from a nozzle by its own vapor pressure. Iso-butane, which is the most promising fuel, has a vapor pressure of about 0.25 MPa (gauge pressure) at room temperature, and needs 31 times larger volume of air than itself for complete combustion.

The basic characteristics of an ejector is figured out from the continuity of fluid, momentum conservation and energy conservation. The continuity of fluid is described by

$$\rho_1 u_1 A_1 + \rho_2 u_2 A_2 = \rho_3 u_3 A_3 \quad (2)$$

where ρ_n is the density of the fluid, u_n the flow velocity, and A_n is the cross-sectional area of a flow channel. Subscripts $n = 1$, 2 and 3 represent the primary, secondary and mixed flow, respectively. The momentum conservation equation is given by

$$(P_1+\rho_1 {u_1}^2)A_1+(P_2+\rho_2 {u_2}^2)A_2 = (P_3 + \rho_3 {u_3}^2)A_3 \quad (3)$$

where P_n is static pressure (gauge pressure). The energy conservation equation is given by

$$\rho_1 |u_1| A_1 \left\{ \frac{v}{v-1}\frac{P_1+P_a}{\rho_1} + \tfrac{1}{2}{u_1}^2 \right\} + \rho_2 |u_2| A_2 \left\{ \frac{v}{v-1}\frac{P_2+P_a}{\rho_2} + \tfrac{1}{2}{u_2}^2 \right\} = \rho_3 |u_3| A_3 \left\{ \frac{v}{v-1}\frac{P_3+P_a}{\rho_3} + \tfrac{1}{2}{u_3}^2 \right\} \quad (4)$$

where v is the ratio of specific heats, and P_a is the atmospheric pressure. From these equations, ejector efficiency, η_e, which is defined as the ratio of the secondary flow to the primary flow, $\eta_e = \rho_2 u_2 A_2 / \rho_1 u_1 A_1$, is calculated. Fig. 4 shows the ejector efficiency, η_e, as a function of relative suction area defined as $\alpha_s = A_1/A_2$. This figure reveals that η_e increases monotonously with increase in α_s when back pressure, P_3, is zero, but α_s should be optimized to maximize η_e unless the back pressure is negligible. Fig. 5 shows the relationship between the density of the primary flow, ρ_1, and the ejector efficiency, η_e. The ejector efficiency degrades with decrease in the density of the primary flow, especially when the back pressure is applied. Therefore, the ejector is useful for heavy gases such as butane.

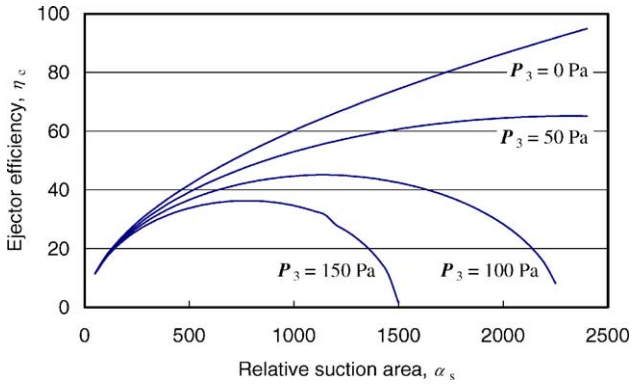

Fig. 4. Relationship between ejector efficiency, η_e, and relative suction area, α_s.

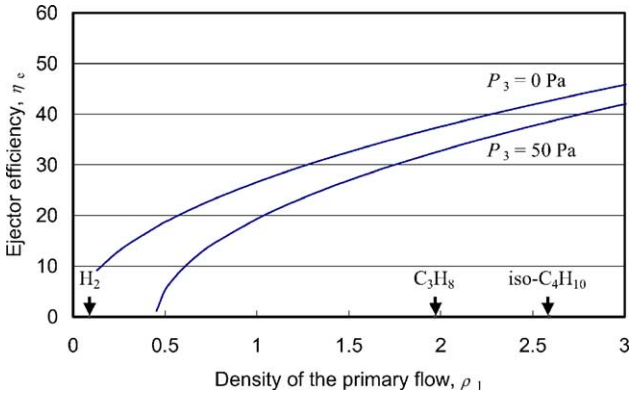

Fig. 5. Relationship between the density of the primary flow, ρ_1, and ejector efficiency, η_e.

Fig. 6 shows the structure of the prototyped micro-ejector. The micro-ejector is manufactured by covering flow channels, which is fabricated on a silicon substrate by three times deep RIE, with a Pyrex glass substrate by anodic bonding. The nozzle is a Laval nozzle to realize a supersonic flow. For test, the primary flow was fed to the micro-ejector from a gas container through a pressure regulator and a mass flow meter. The flow rate of the mixed flow was measured using a soap film flow meter with low pressure loss. The back pressure is adjusted using a choke valve at the exit of the micro-ejector. The experimental results of each prototype are shown in Figs. 7 and 8, where relative suction area, α_S, and used primary flow are displayed. When butane was used as a primary flow, and the back pressure was zero, an ejector efficiency of 31.2 was achieved, satisfying the requirement ($\eta_e > 31$). Fig. 9 shows the maximum ejector efficiency,

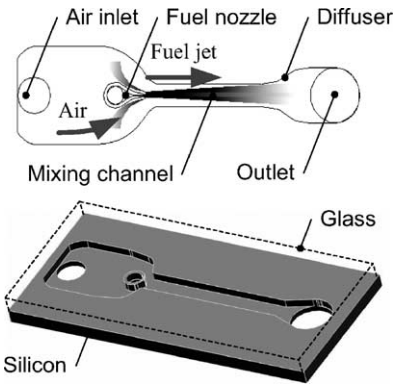

Fig. 6. Structure of the prototyped micro-ejector.

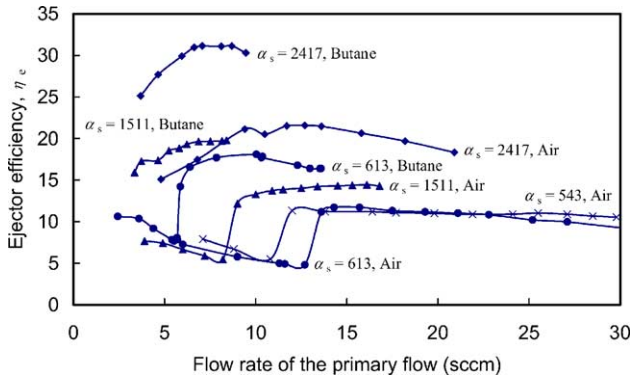

Fig. 7. Relationship between the flow rate of the primary flow and ejector efficiency, η_e.

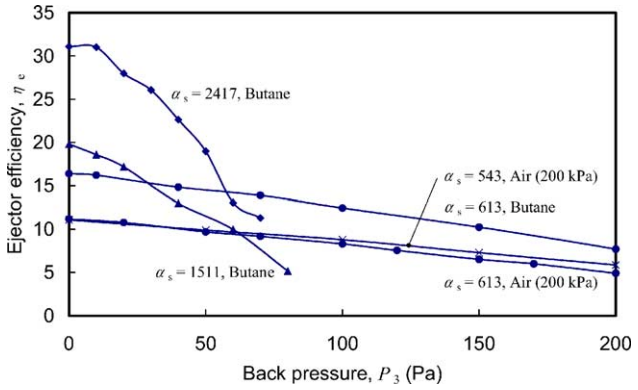

Fig. 8. Relationship between back pressure and ejector efficiency, η_e.

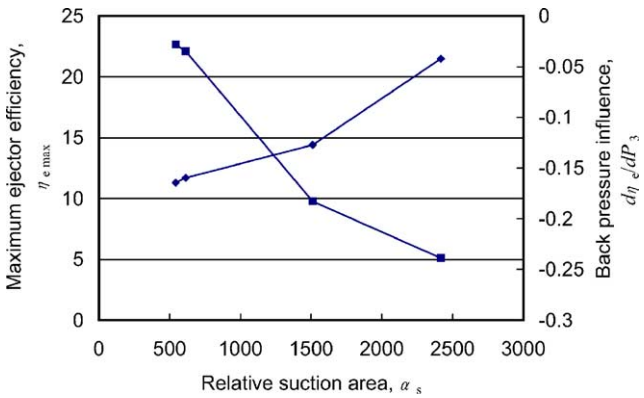

Fig. 9. Maximum ejector efficiency, $\eta_{e,max}$, and the influence of back pressure, $d\eta_e/dP_3$, as functions of relative suction area, α_s (the primary flow is air).

$\eta_{e,max}$, and the influence of the back pressure represented by the gradient of each line in Fig. 8, $d\eta_e/dP_3$, as functions of α_s (the primary flow is air). There seems the tradeoff tendency that $\eta_{e,max}$ increases, but the insensitivity to the back pressure, $d\eta_e/dP_3$, decreases with increase in α_s. The flow rate of the prototypes used in this study matches 20 W class combustion of butane. For low power applications such as portable information devices, the micro-ejector should be tuned for lower flow rate.

5. Catalytic micro-butane combustor

Hydrogen is often used for combustion at micro-scale, because hydrogen is easiest to burn in a small volume, as indicated by its small quenching distance. Methanol is also highly reactive and suited for combustion at micro-scale. Liquid gases such as butane and propane, however, are not like hydrogen and methanol. We think that butane is the most promising fuel for portable power sources, because its moderate vapor pressure around 0.2–0.25 MPa (gauge pressure) allows butane to be stored in a plastic or thin metal cartridge, and butane is already accepted in our society as fuels for table-top cooking burners, disposable lighters and travel hair irons. Thus, we developed a catalytic micro-combustor for butane.

Fig. 10 shows the structure of the micro-combustor. The micro-combustor has a combustion chamber of 14 mm × 8 mm × 0.15 mm (depth) anisotropically wet-etched in a silicon substrate and covered with an anodically bonded Pyrex glass substrate with gas ports. Platinum-loaded TiO_2 catalyst is embedded in the micro-combustor by the above-mentioned method. For test, fuel and air were supplied to the micro-combustor through mass flow controllers, and exhausted gas was analyzed by gas chromatography. Combustion was initiated by heating the micro-combustor by a gas lighter. The pressure loss of the micro-combustor was measured, after the exit was disconnected from the gas chromatography system and opened to atmosphere. The temperature distribution of the micro-combustor was observed using an infrared imager (TVS-8500, Avionics).

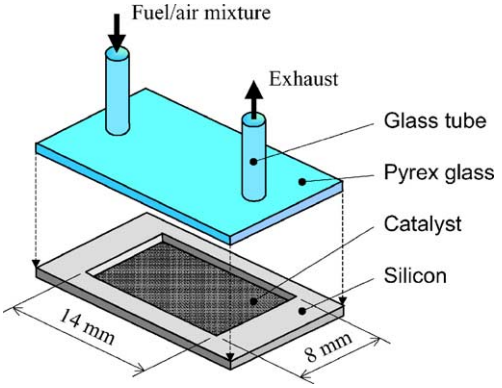

Fig. 10. Structure of the micro-combustor.

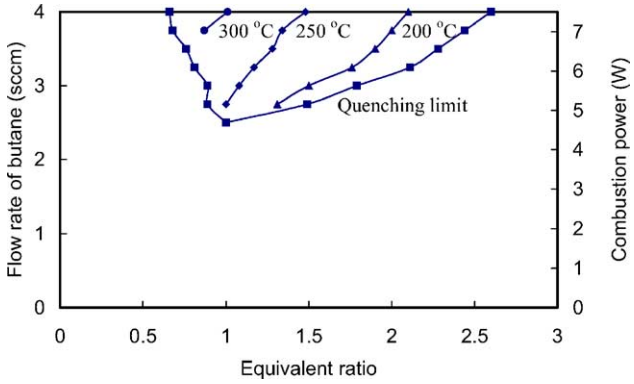

Fig. 11. Stable combustion area of the micro-combustor.

Fig. 11 shows a stable combustion area, whose horizontal and vertical axes represent equivalent ratio and the flow rate of butane, respectively. The power obtained by the complete combustion of supplied butane is also plotted on the right vertical axis. Temperature contours shown in Fig. 11 represent peak temperature measured by the infrared imager. As shown in this figure, quenching is occurred by reducing the flow rate of butane, because heat dissipation overcomes heat generation. The minimum power at which we confirmed stable combustion is 5 W under the assumption that butane was completely burned. Gas chromatography detected no unburned fragments such as CO and hydrocarbons, when 4 sccm butane was supplied at an equivalent ratio of 1, suggesting the achievement of complete combustion. However, a hot zone was localized around the gas inlet, and controlling the temperature distribution is one of future challenges.

Fig. 12 shows the pressure loss of the micro-combustor. This figure displays three lines obtained by calculation, measurement using air and measurement with combustion using air and hydrogen (8 sccm). To use the micro-ejector, the pressure loss must be reduced to a few tens Pa. To satisfy this requirement, however, these prototypes should limit the flow rate of mixed gas to as low as 20–30 sccm. The pressure loss should be decreased by increasing the depth of the combustion chamber or an opened area at the exit.

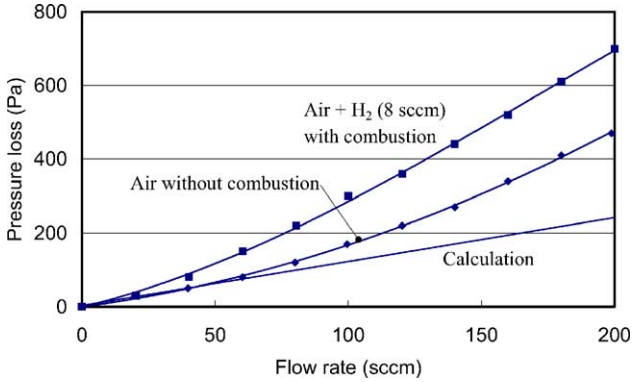

Fig. 12. Pressure loss of the micro-combustor.

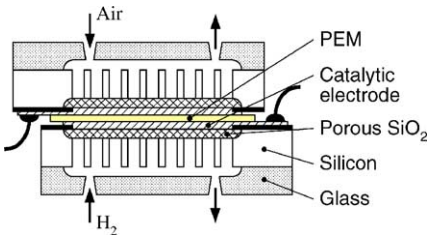

Fig. 13. Structure of the MEMS-based PEFC.

6. MEMS-based polymer electrolyte fuel cell

Wafer level batch process is useful to produce micro-devices. This is also true for micro-fuel cells with very small cell size. Fig. 13 shows the structure of a MEMS-based PEFC. Catalytic electrodes, gas diffusion layers and gas channels are formed on a silicon/glass substrate by MEMS technology. The fabrication process is as follows. First, a Si_3N_4 mask is patterned on a silicon substrate, and unmasked silicon is anodized into porous silicon in a solution containing HF and ethanol. Subsequently, the porous silicon is thermally oxidized at 900 °C. Next, gas feed holes are fabricated from the back side of the silicon substrate by deep RIE, and then a Pyrex glass substrate with a gas channel and gas ports is anodically bonded to the silicon substrate. The catalytic electrode is a platinum thin film sputtered through a shadow mask or screen-printed platinum-loaded carbon. Screen-printing paste is made by loading platinum on carbon black using $[Pt(NH_3)_4]Cl_2$ solution and then mixing the carbon black with PTFE power, the ethanol solution of polymer electrolyte and dibutyl phthalate. Finally, a polymer electrolyte membrane (PEM) (Flemion S, Asahi glass, 80 μm thick) is sandwiched between the silicon substrates by hot pressing.

Fig. 14 shows the output characteristics of a prototype with 300 nm thick sputtered platinum catalytic electrodes. Sudden voltage drop from open circuit voltage suggests low catalytic activity, and subsequent voltage drop at current density of several hundreds $\mu A/cm^2$ suggests very large internal resistance. The latter may be mainly due to poor adhesion between the catalytic electrodes and the PEM. The adhesion further deteriorated during test, so that the power density decreased to several tens $\mu W/cm^2$, because the PEM swelled by produced water. Of course, mechanically clamping is easy to improve the adhesion, but is not practical nor preferable from the view-point of size. Further effort is necessary to improve the adhesion.

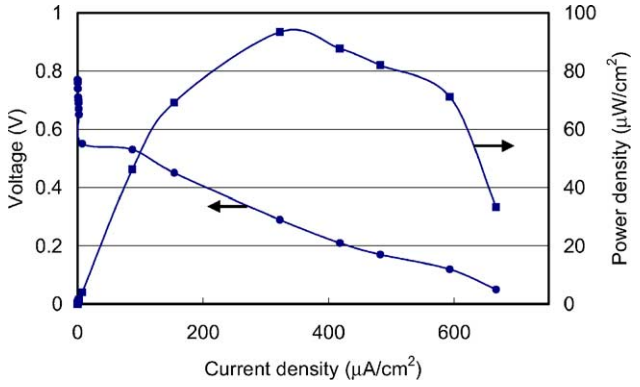

Fig. 14. Output characteristics of the prototyped MEMS-based PEFC.

7. Conclusion

In this paper, we proposed a novel miniature fuel cell/fuel reformer system fueled by liquid gases such as butane and propane. In this system, fuel, air and water are supplied to the micro-fuel reformer by utilizing the vapor pressure of the liquid gas for the reduction of power consumption by peripherals and the simplification of the system. In this study, we prototyped micro-ejectors to supply air to a micro-combustor by MEMS technology, and confirmed that it had a potential to supply air required for the complete combustion of butane (31 times larger volume than butane).

We also prototyped a combustor-integrated micro-fuel reformer with a suspended membrane structure, a catalytic micro-combustor for butane and a MEMS-based polymer electrolyte fuel cell (PEFC). The micro-fuel reformer demonstrated the steam reforming of methanol at an equivalent power of 200 mW and a total efficiency of 6%. The micro-combustor had a stable combustion area above 5 W, and the complete combustion of butane was confirmed by gas chromatography. The MEMS-based PEFC worked, but only at low power density of about 0.1 mW/cm^2 due to poor adhesion between a polymer electrolyte membrane (PEM) and catalytic electrodes.

Acknowledgements

This work was partly supported by the New Energy and Industrial Technology Development Organization (NEDO) of Japan.

References

[1] A.H. Epstein, Millimeter-scale, MEMS gas turbine engines, in: Proceedings of the ASME Turbo Expo 2003, Power for Land, Sea, and Air, Atlanta, GA, USA, 2003, GT-2003–38866.

[2] K. Isomura, S. Tanaka, M. Murayama, H. Yamaguchi, N. Ijichi, T. Genda, N. Saji, O. Shiga, K. Takahashi, M. Esashi, Development of micro-turbo charger and micro-combustor as feasibility studies of three-dimensional gas turbine at micro-scale, in: Proceedings of the ASME Turbo Expo 2003, Power for Land, Sea, and Air, Atlanta, GA, USA, 2003, GT-2003–38151.

[3] S. Tanaka, K. Isomura, T. Kato, F. Sato, M. Oike, T. Genda, M. Hara, T. Kamatsuchi, S. Sugimoto, J -F. Li, H. Yamaguchi, N. Ijichi, M. Murayama, K. Nakahashi, M. Esashi, Design and fabrication challenges for micro-machined gas turbine generators, in: Proceedings of the Ninth International Symposium on Transport Phenomena and Dynamics of Rotating Machinery (ISROMAC-9), Honolulu, HI, USA, 2002.

[4] S. Kang, J.P. Johnston, T. Arima, M. Matsunaga, H. Tsuru, F.B. Prinz, Micro-scale radial-flow compressor impeller made of silicon nitride—matufacturing and performance, in: Proceedings of the ASME Turbo Expo 2003, Power for Land, Sea, and Air, Atlanta, GA, USA, 2003, GT-2003–38933.
[5] J.D. Morse, A.F. Jankowski, R.T. Graff, J.P. Hayes, Novel proton exchange membrane thin-film fuel cell for micro-scale energy conversion, J. Vac. Sci. Technol. A 18 (4) (2000) 2003–2005.
[6] K.-B. Min, S. Tanaka, M. Esashi, MEMS-based polymer electrolyte fuel cell, Electrochemistry 70 (12) (2002) 924–927.
[7] K.-B. Min, S. Tanaka, M. Esashi, Silicon-based micro-polymer electrolyte fuel cells, in: Proceedings of the IEEE 16th Annual International Conference on Microelectro Mechanical Systems, Kyoto, Japan, 2003, pp. 379–382.
[8] S.J. Lee, A. Chang-Chien, S.W. Cha, R. O'Hayre, Y.I. Park, Y. Saito, F.B. Prinz, Design and fabrication of a micro-fuel cell array with "flip-flop" inter connection, J. Power Sour. 112 (2002) 410–418.
[9] A. Heinzel, C. Hebling, M. Müller, M. Zedda, C. Müller, Fuel cell for low power applications, J. Power Sour. 105 (2002) 250–255.
[10] T. Yoshitake, Small direct methanol fuel cell pack for portable applications, Electrochemistry 70 (12) (2002) 966–968.
[11] J.D. Holladay, E.O. Jones, M. Phelps, J. Hu, Microfuel processor for use in a miniature power supply, J. Power Sour. 108 (2002) 21–27.
[12] K.S. Chang, S. Tanaka, M. Esashi, Combustor-integrated micro-fuel processor with suspended membrane structure, in: Proceedings of the 12th International Conference on Solid-state Sensors, Actuators and Microsystems, Digest of Technical Papers, Transducers '03, Boston, MA, USA, 2003, pp. 635–638.
[13] L.R. Arana, C.D. Basertsch, R.C. Schmidt, M.A. Schmidt, K.F. Jensen, Combustion-assisted hydrogen production in a high temperature chemical reactor/heat exchanger for portable fuel cell applications, in: Proceedings of the 12th International Conference on Solid-state Sensors, Actuators and Microsystems, Digest of Technical Papers, Transducers '03, Boston, MA, USA, 2003, pp. 1734–1737.
[14] S.B. Schaevitz, A.J. Franz, K.F. Jensen, M.A. Schmidt, Combustion-based MEMS thermoelectric power generator, in: Proceedings of the 11th International Conference on Solid-state Sensors and Actuators, Digest of Technical Papers, Transducers '01, Eurosensors XV, Munich, Germany, 2001, pp. 30–33.
[15] C. Zhang, K. Najafi, L.P. Bernal, P.D. Washabaugh, An integrated combustor-thermoelectric micro power generator, in: Proceedings of the 11th International Conference on Solid-state Sensors and Actuators, Digest of Technical Papers, Transducers '01, Eurosensors XV, Munich, Germany, 2001, pp. 34–37.
[16] O.M. Nielsen, L.R. Arana, C.D. Baertsch, K.F. Jenson, M.A. Schmidt, A thermophotovoltaic micro-generator for portable power applications, in: Proceedings of the 12th International Conference on Solid-state Sensors, Actuators and Microsystems, Digest of Technical Papers, Transducers '03, Boston, MA, USA, 2003, pp. 714–717.
[17] C. Zhang, K. Najafi, L.P. Bernal, P.D. Washabaugh, Micro combustion-thermoionic power generation: feasibility, design and initial results, in: Proceedings of the 12th International Conference on Solid-state Sensors, Actuators and Microsystems, Digest of Technical Papers, Transducers '03, Boston, MA, USA, 2003, pp. 40–44.